

Exploratory analysis of an optimal variable speed control system for a recurrently congested freeway bottleneck

Xianfeng Yang*, Yang (Carl) Lu and Gang-Len Chang

Department of Civil and Environmental Engineering, University of Maryland, College Park, MD, 20742, USA

SUMMARY

This study presents two models for proactive variable speed limit (VSL) control on a recurrently congested freeway segment. The proposed model uses embedded traffic flow relations to predict the evolution of congestion patterns over the projected time horizon, and then computes the time-varying optimal speed limit to smooth traffic flows. To contend with the uncertainties associated with drivers' responses to VSL control, this study has also proposed an advanced model that further adopts Kalman Filter to enhance the traffic state estimation. Both models have been investigated with two control objectives—travel time minimization and speed variance minimization. Our extensive simulation analysis with a VISSIM simulator, calibrated with field data from our previous VSL field demonstration, has revealed the benefits of the proposed VSL control models. Also, the experimental results indicated that the proposed advanced models with both control objectives can significantly reduce the travel time over the recurrent bottleneck locations. With respect to several selected measure of effectiveness (MOEs), such as average number of stops and average travel time, the research results confirm that the control models with the objective of minimizing speed variance can offer the promising properties for field implementation. Copyright © 2014 John Wiley & Sons, Ltd.

KEY WORDS: variable speed limit; optimal control; Kalman Filter; traffic flow model

1. INTRODUCTION

Recurrent congestion on freeway segments around major metropolitan areas is becoming even more severe over the recent decades. The formation of traffic queues at recurrently congested bottlenecks often prevents motorists from fully utilizing the capacity of existing freeway infrastructure. However, building a new highway has been becoming increasingly difficult because of the diminishing resources for infrastructure construction. Hence, some operations strategies, such as ramp metering [1–4] and variable speed limit (VSL) control, have evolved to be promising control methods since the emergence of Intelligent Transportation System (ITS) in 1990s.

The VSL is initially designed to reduce the speed difference on some hazardous highway segments so as to decrease the rear-end collisions and improve traffic safety [5–7]. Recently, it has been recognized that VSL may also offer the potential to mitigate traffic congestion and improve traffic efficiency at work-zones and freeway bottlenecks. Through dynamically changed speed limits along a controlled segment, VSL can smooth the speed transition between the upstream and congested downstream flows to minimize the impact of shockwaves on traffic conditions. The mitigation of traffic speed variance can also facilitate traffic flows to better utilize the available roadway capacity during peak periods.

Focusing on the work-zone safety, a set of studies has further considered to improve traffic efficiency with the VSL control logic (Michigan Department of Transportation [8], Lin *et al.* [9], Kang *et al.* [10], Kang [11], Kwon *et al.* [12], and Fudala and Fontaine [13]). Despite the potential benefits of VSL for work-zone conditions, most of such systems are exploratory in nature, using relative primitive methods. Hence, design of reliable algorithms to ensure its benefits in recurrent congestion remains a challenging issue.

*Correspondence to: Xianfeng Yang, Department of Civil and Environmental Engineering, University of Maryland, College Park, MD, 20742, USA. E-mail: xyang125@umd.edu

With respect to VSL for recurrent congestion, most existing studies were conducted in simulated environments. For example, Abdel-Aty *et al.* [14, 15] developed a VSL system for I-4 through Orlando, Florida, where relatively simple control strategy was adopted to minimize the difference between the speed limit and current average speed. Their study reported the reduction in both crash risk and travel time under a simulated environment. However, because the main control objective was to improve safety measurement, their savings of travel time was marginal. Hegyi *et al.* [16, 17] modified the METANET traffic flow model and incorporated the VSL effect with the model predictive control (MPC) approach to determine the optimal speed limit. Nearly 20% of travel time reduction has been reported in their case studies, where the incoming flow rates were assumed to be constant during the simulation period. Papageorgiou *et al.* [18] and Carlson *et al.* [19] analyzed the effect of VSL on aggregated traffic flow behavior from the theoretical perspective and proposed an open-loop integrated optimal control framework to coordinate ramp metering with VSL control. Their simulation results showed an improvement in total travel time by 15% if the data for demand patterns are quite reliable. For potential field applications, they further developed a two-loop local feedback controller to decide the VSL speed, which yields comparable result in a METANET simulation environment [20]. Using a modified CTM model, Hadiuzzaman and Qiu [21] proposed a VSL control along with the MPC method to dynamically change the speed limit during the operations. Their VISSIM simulation assumed that detectors were placed at every cell to obtain the initial traffic state as the input for MPC, and the results showed a reduction of 15% in total travel time. More recently, Talebpour *et al.* [22] proposed a reactive rule-based speed harmonization strategy to delay or even prevent the traffic breakdown and conducted a simulation experiment to support the algorithm's effectiveness in terms of improving both safety and efficiency. Their study assumed that connected vehicle technologies are available to obtain each vehicle's trajectory and to facilitate the early detection of shockwaves.

With respect to VSL field deployment, most of such systems are conducted in Europe, and the resulting performance varies with each VSL system's embedded algorithm. For example, the VSL experiment in Dutch [23] showed no improvement in capacity, which may be attributed to its advisory nature. Hegyi and Hoogendoorn [24] developed the SPECIALIST algorithm to operate the variable speed limit, which is designed explicitly to resolve the shockwaves based on a reactive manner. A field evaluation in Dutch A12 freeway [24] showed that such a function can significantly mitigate the impact of shockwaves, but not reduce the total travel time. Weikl *et al.* [25] analyzed the data obtained from German Autobahn A99 near Munich, and concluded that VSL could reduce the shockwave speed and balance the lane distribution at the cost of slightly reduced capacity. In the US, Chang *et al.* [26] reported a successful demonstration of an integrated VSL and travel time information system on MD 100 near Coca-Cola Drive, which found that pairing VSL with a displayed travel time system can significantly reduce the travel time and increase the throughput over the bottleneck segment.

In brief, most proactive models can outperform reactive control algorithms in terms of improving traffic flow efficiency. However, some vital technical issues remain to be addressed prior to the comprehensive implementation of proactive VSL control methods. For instance, the traffic flow model, adopted for traffic state estimation/prediction, may not reliably capture dynamic interactions between all essential system components, such as the blockages at weaving areas and drivers' non-compliance to the VSL system. The selected control objective may also affect the performance of a VSL system. Hence, this study has presented not only a predictive VSL model, but also enhance our proposed model with a Kalman filter algorithm that enables the VSL system to constantly update the traffic states produced from the embedded traffic flow models, based on the difference between the previously predicted traffic states and detected conditions from field traffic sensors. To explore the impacts of a selected control objective on the VSL's effectiveness, this study has also investigated two control objectives with both the base and enhanced models, which are total travel time minimization and speed variance minimizations.

This paper is organized as follows: The key features of the proposed VSL system are briefly described in the next section. Formulations of the basic proactive model are introduced in Section 3. Section 4 addresses the design of the traffic state estimator, based on the Kalman filtering methodology, followed by presentation of the enhanced VSL model. Design of simulation experiments for the performance evaluation under simulated real-time control environments is reported in Section 5. Conclusions and future research are summarized in the last section.

2. VSL SYSTEM DESCRIPTION

As shown in Figure 1, approaching vehicles from upstream segments due to congestion are often forced to slow down before reaching the bottleneck. The formation of bottleneck may be caused by various factors, such as lanes reduction or weaving maneuvers from heavy ramp flows. Without proper control, the approaching vehicles are likely to slow their speeds abruptly just upstream of the bottleneck location, thus often dropping from a high-speed (e.g. free-flow speed) to ‘stop-and-go’ conditions and consequently producing shockwaves to reduce the throughput as well as the speed over the bottleneck segment. The VSL proposed in this study is designed to mitigate such impacts so as to best use the available capacity of the congested segment.

The proposed VSL system consists of detectors, variable speed limit signs, and a central processing unit to execute control actions. The upstream detector in Figure 1 is used to capture the arrival flow rate, and the downstream detector is designed to record the discharging rate from the bottleneck. Also, additional detectors are placed at those on-ramps and off-ramps to record ramp arriving and departing flows. Several VSL signs along with detectors would be installed between the upstream and downstream detectors. In a field application, those VSL signs shall dynamically update their displayed speed limit based on the computed optimal set of speeds and the specified criteria for VMS display.

Depending on the approaching volume, drivers’ compliance rate, and the resulting congestion along the target freeway segment, a VSL system’s central processing unit is responsible to produce the time-varying optimal speed limits. Note that for the safety concern and effective communications with drivers, all displayed speed limits are supposed to remain unchanged over a specified control horizon.

3. BASIC PROACTIVE CONTROL MODEL

The operational structure of the proposed VSL control system includes the following two principal components:

- Traffic state model: Given the detected upstream flow rate, the on-ramp and off-ramp flow rate, and the downstream discharging rate, the model will function to predict the traffic state evolution in each freeway subsection;
- Optimization model: Based on the estimated conditions from embedded traffic flow model, the system will execute the optimization model to predict the traffic state in the next prediction horizon and yield the set of optimal speed limits.

For convenience of discussion, the control variables and parameters are listed in succeeding text:

- Control time and subsection index
 - ΔT : Unit time interval to update the traffic flow model;
 - T^P : Time interval for prediction horizon;
 - T^C : Time interval for control horizon;
 - k : Time interval index for the discrete traffic flow model;
- Network geometric and physical data
 - ΔL : Length of each freeway segment;
 - n_i : Number of lanes in subsection i ;

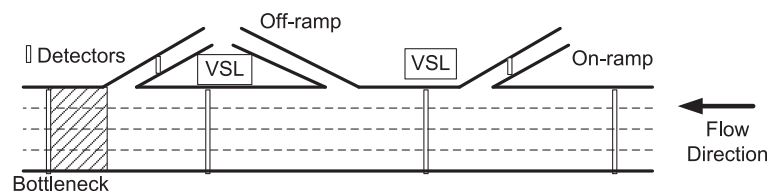


Figure 1. Configuration of a variable speed limit system.

- Traffic states variables
 - $q_i(k)$: Transition flow rate entering segment $(i + 1)$ from segment i during interval k ;
 - $r_i(k)$: On-ramp flow rate entering segment i during interval k ;
 - $s_i(k)$: Off-ramp flow rate leaving segment i during interval k ;
 - $d_i(k)$: Mean traffic density per lane in segment i during interval k ;
 - $u_i(k)$: Mean speed in segment i during interval k ;
- Control variables, boundaries and model parameters
 - $v_i(k)$: Variable speed limit ratio in segment i during interval k ;
 - d_j : Jam traffic density;
 - d_c : Critical traffic density;
 - u_f : Free flow speed;
 - δ : Maximum allowable difference for VSL change
 - v, τ, κ, a : Traffic state model parameters;

3.1. Macroscopic traffic flow model

To perform a proactive dynamic VSL control, a reliable prediction model is essential to predict the traffic state evolution under the detected traffic conditions and driver responses. This study employs a calibrated traffic flow model to predict traffic conditions over the target time horizon, and to provide the information for activating the VSL optimization module.

As shown in Figure 2, the target freeway segment is conceptually divided into N subsections with a unit length of ΔL . While dividing a freeway segment into subsections, the length of each subsection should be sufficiently long so that vehicles cannot pass one subsection during one-time interval k . Moreover, each subsection is allowed to have at most one on-ramp and one off-ramp. For each subsection i , the mean density, $d_i(k)$, can be determined by the difference between the input and output flows as follows:

$$d_i(k + 1) = d_i(k) + \frac{\Delta T}{\Delta L * n_i} [q_{i-1}(k) - q_i(k) + r_i(k) - s_i(k)] \quad (1)$$

For dynamically updating the average speed, $u_i(k)$, a well-developed equation proposed by the METANET model [27] is adopted and shown as follows:

$$u_i(k + 1) = u_i(k) + \frac{\Delta T}{\tau} \{V[d_i(k)] - u_i(k)\} + \frac{\Delta T}{\Delta L} u_i(k) [u_{i-1}(k) - u_i(k)] - \frac{v \cdot \Delta T}{\tau \cdot \Delta L} \frac{d_{i+1}(k) - d_i(k)}{d_i(k) + \kappa} \quad (2)$$

where, $V[d_i(k)]$ is the static speed for segment i at time k with respect to the density $d_i(k)$:

$$V[d_i(k)] = u_f \cdot \exp \left[-\frac{1}{a} \left(\frac{d_i(k)}{d_c} \right)^a \right] \quad (3)$$

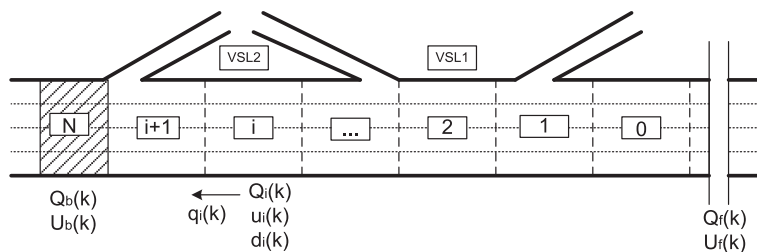


Figure 2. Typical freeway segments.

Also, the relationship between flow, density, and speed is given by the following:

$$q_i(k) = d_i(k)u_i(k)n_i \quad (4)$$

Using the detected inflow rate from the upstream and on-ramp detectors, one can directly use Equations 1–4 to estimate and predict the traffic state evolution at the target freeway segment.

3.2. Optimization model with prediction

Based on the traffic state at current time interval, one can further implement the traffic flow model (Equations 1–4) to predict the traffic state within the next prediction horizon with respect to different speed limits. Then, the one with the best objective output can be selected for implantation. Hence, the first step of the optimization model is to select a proper control objective function.

As the primary focus of VSL is to increase traffic flow speed and its stability, this study first adopts the following objective of minimizing of total travel time over the controlled segment:

$$\min \sum_k \sum_i n_i d_i(k) \Delta T \quad (5)$$

Note that depending on the response of drivers to the displayed speeds, the embedded macroscopic traffic flow models and the aforementioned objective function may not fully capture the complex traffic dynamics and yield the true optimal results.

As reported in the literature [5–7], a proper VSL control can help smooth speed transition and consequently reduce the number of vehicle stops and shockwave impact on the traffic conditions [26]. Hence, this study has further explored the following objective function of minimizing the speed variance along the target freeway for a VSL control:

$$\min \sum_k \sum_i (u_i(k) - u_{ave})^2 \quad (6)$$

where, u_{ave} is the average speed of the target freeway stretch, and is given as follows:

$$u_{ave} = \frac{\sum_k \sum_i u_i(k)}{(T^c / \Delta T) \cdot N} \quad (7)$$

To implement the optimization model and select the proper control speed limit for the projected control period, one shall place the following additional constraints.

For each subsection i , its mean speed shall not exceed the displayed speed limit:

$$\begin{cases} u_j \leq u_i(k) \leq u_f, & \text{segment } i \text{ without VSL control;} \\ u_j \leq u_i(k) \leq u_f v_i(k), & \text{segment } i \text{ with VSL control.} \end{cases} \quad (8)$$

where,

$$0 < v_i(k) \leq 1 \quad (9)$$

One shall also set the density boundaries to reflect the jam density constraint as follows:

$$0 \leq d_i(k) \leq d_j \quad (10)$$

Also, for safety concern, the speed variation between consecutive intervals shall be set within the following boundaries.

$$-\delta \leq u_i^f v_i(k) - u_i^f v_i(k-1) \leq \delta \quad (11)$$

where, δ is the maximum allowable difference between two successive speeds displayed on VMS.

Note that the speed variation between consecutive intervals shall be limited within a given range, as shown in 11. Therefore, the feasible solution set is quite small and one can thus adopt enumerative search for the optimal solution.

4. ENHANCED PROACTIVE CONTROL MODEL

In reality, the freeway congestion may be caused by many factors aside from an increase in traffic demand. For example, traffic weavings can result in the formation of bottlenecks. Therefore, because of the limitation of macroscopic traffic flow models, this study has further adopted the Kalman Filter, which has been proved to be effective for model updating in real-time operations [28]. Kalman Filter is an optimal state estimator applied to a dynamic system that involves random noise and includes a limited amount of noisy real-time measurements. The correction and update process of a typical Kalman Filter process is summarized in Figure 3:

where, $\mathbf{y}(k)$ is the estimated traffic state vector:

$$\mathbf{y}(k) = [q_1(k) \ u_1(k) \ q_2(k) \ u_2(k) \ \cdots \ q_N(k) \ u_N(k)]^T \quad (12)$$

And $\mathbf{u}(k)$ is the system input:

$$\mathbf{u}(k) = [q_0(k) \ v_0(k) \ q_{N+1}(k) \ v_{N+1}(k) \ r_1(k) \ \cdots \ r_N(k) \ s_1(k) \ \cdots \ s_N(k)]^T \quad (13)$$

Also, $f(\cdot)$ represents the traffic flow model shown by Equations 1–4; and $\mathbf{z}(k)$ denotes the vector of measurements. In a typical VSL system shown in Figure 1, it collects three types of measurements in real time, including freeway flow rate, freeway speed, and on-ramp flow rate.

The measurements $\mathbf{z}(k)$ has the following relation with $\mathbf{x}(k)$:

$$\mathbf{z}(k) = h(\mathbf{y}(k), \mathbf{v}(k)) \quad (14)$$

where, $\mathbf{v}(k)$ is the measurement error.

Four important matrices involved in the computations are shown in the succeeding text:

\mathbf{A} is the Jacobian matrix of partial derivatives of function $f(\cdot)$ with respect to x :

$$\mathbf{A}_{[i,j]} = \frac{\partial f_{[i]}}{\partial y_{[j]}}(\mathbf{y}(k-1), \mathbf{u}(k-1), 0) \quad (15)$$

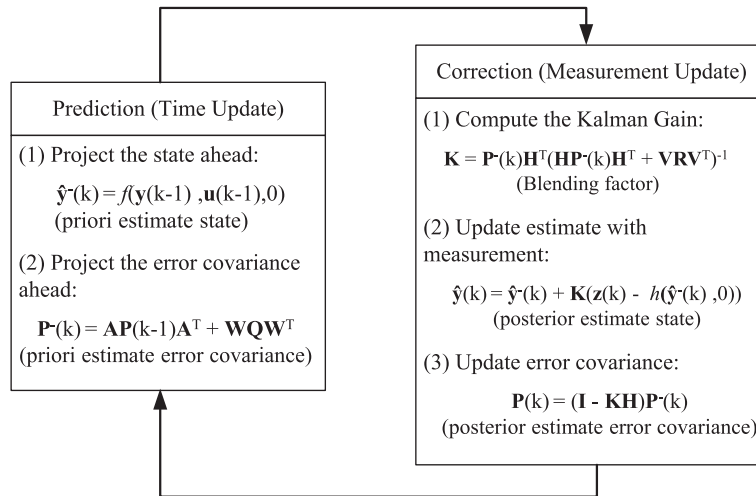


Figure 3. An Illustration of Kalman Filter Correction and Update Process.

\mathbf{W} is the Jacobian matrix of partial derivatives of function $f(\cdot)$ with respect to process noise w :

$$\mathbf{W}_{[i,j]} = \frac{\partial f_{[i]}}{\partial w_{[j]}}(\mathbf{y}(k-1), \mathbf{u}(k-1), 0) \quad (16)$$

\mathbf{H} is the Jacobian matrix of partial derivatives of function $h(\cdot)$ with respect to x :

$$\mathbf{H}_{[i,j]} = \frac{\partial h_{[i]}}{\partial y_{[j]}}(\mathbf{y}(k), \mathbf{v}(k)) \quad (17)$$

\mathbf{V} is the Jacobian matrix of partial derivatives of function $h(\cdot)$ with respect to measurement noise v :

$$\mathbf{V}_{[i,j]} = \frac{\partial h_{[i]}}{\partial v_{[j]}}(\mathbf{y}(k), \mathbf{v}(k)) \quad (18)$$

By using the Kalman Filter, the traffic state at current time interval can be constantly updated based on the detector data, and the new optimal speed limits can then be generated with the prediction function in the optimization model.

As mentioned in Section 2, to avoid confusing drivers, the displayed speed limits are not allowed to change frequently. Therefore, by defining a control horizon T^C , the speed limits will remain unchanged over the specified time interval. Also note that the optimization model will be activated once all detector data have been updated, where the control horizon is normally set to equal the length of multiple detector update intervals. Therefore, during each control horizon, the optimization model will produce multiple estimates of the optimal speed limit, and the process to select the robust one prior to its execution is shown in the succeeding text.

For example, assuming that both control horizon and prediction horizon are set to be 5 minutes and the detector data is updated at an interval of every minute, then each control interval will have five sets of estimated optimal speed limits prior to its implementation time, as shown in Figure 4.

Given the set of computed optimal speed limits for the same horizon, $\{v(1), v(2), \dots, v(n)\}$, one can determine the speed limits to be displayed based on the following procedure:

- (1) Define a counter M to identify the moving direction of the speed limit, and then denote v^t as the displayed speed limit of the current horizon, where M is updated by the following expression:

$$M = \begin{cases} M + 1, & \text{if } v(i) > v^t \\ M, & \text{if } v(i) = v^t, \quad i = 1, 2, \dots, n; \\ M - 1, & \text{if } v(i) < v^t \end{cases} \quad (19)$$

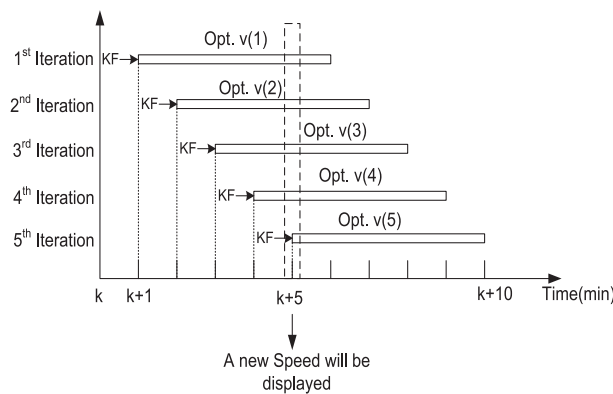


Figure 4. An example of the variable speed limit control strategy.

- (2) The new displayed speed limit for the next horizon will be readjusted with the predetermined increment Δ , based on the value of M :

$$v^{t+1} = \begin{cases} v^t + \Delta, & \text{if } M > 0 \\ v^t, & \text{if } M = 0 \\ v^t - \Delta, & \text{if } M < 0 \end{cases} \quad (20)$$

In summary, the entire proactive control process includes the following primary steps:

- Step 0: Divide the target freeway segment into a set of subsections and then deploy the VSL signs and detectors; determine the length of control time interval.
- Step 1: Apply the Kalman Filter module to revise the predicted traffic conditions produced from the macroscopic traffic model, and execute the optimization model to generate a new set of optimal speed limits for each detector update interval.
- Step 2: Update the counter M by comparing the new optimal speed limit with the current displayed speed; see 19.
- Step 3: Select the new speed limits to display, based on 20.
- Step 4: Stop the VSL operations if traffic flow speed has been recovered to its normal prevailing speed.

The operational flow chart of the VSL control system is presented in Figure 5:

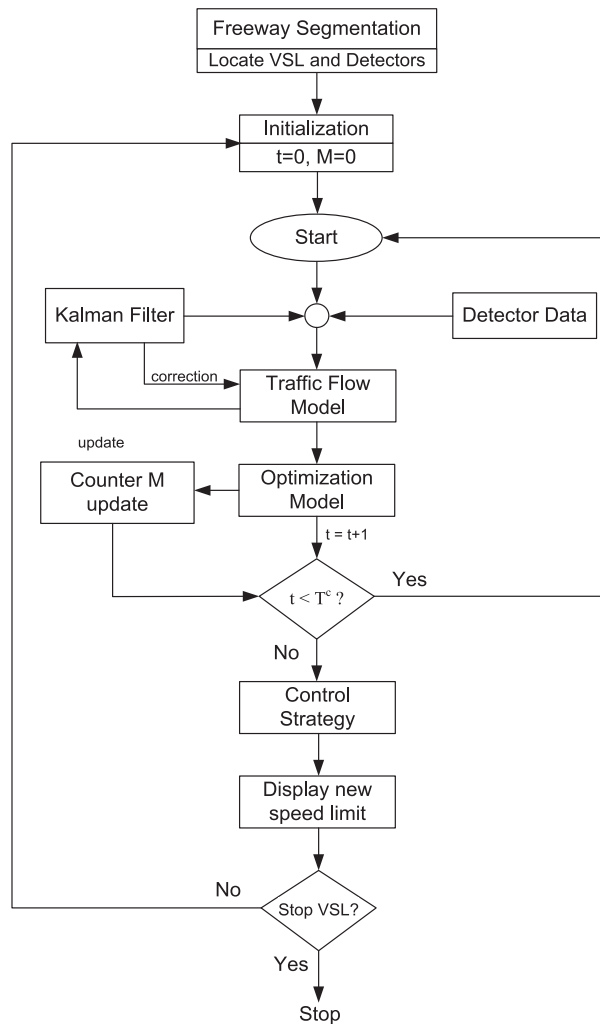


Figure 5. Flow chart of the enhanced proactive model variable speed limit control system.

5. SYSTEM EVALUATION

5.1. Case description

To evaluate the proposed optimization models, this study selected the segment MD-100 West from MD 713 to Coca-Cola Drive, our previous VSL field demonstration site, for simulation analysis. On typical weekdays, the speed during the peak hours usually drops quickly from 60 to 20 mph (e.g., in 5 minutes) after the onset of congestion, and recovers to about 40 mph after passing Coca-Cola Drive. On the selected freeway segment, our research group implemented two VSL signs, four sensors along with License-plate-recognition system on Dec. 2009 to Jan 2010. Using the collected field data, Figure 6(A) illustrates the spatial evolution of traffic flow speeds on the target MD-100 segment. Obviously, a downstream bottleneck is formed near the 295 N off-ramp due to the following contributing factors: (1) the high traffic volume from the 295 N on-ramp can lead to an increase in density on the downstream segments; and (2) the traffic weaving effect caused by 295 N off-ramp volume and 295 N on-ramp volume can significantly impact the vehicle speed due to the short distance between two ramps.

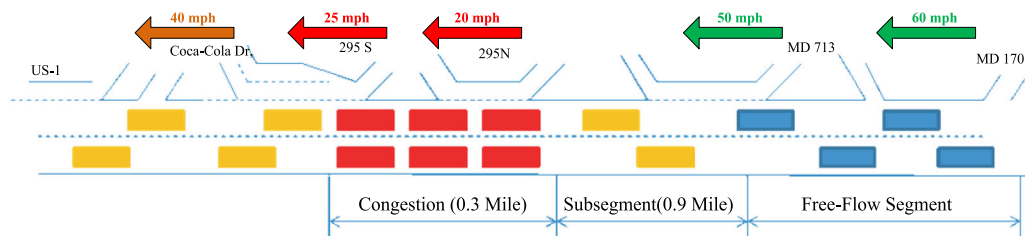
Based on the observed congestion during peak hours, a VSL control system, consisting of one VSL sign, three freeway detectors and four ramp detectors, was installed between MD 713 and Coca-Cola Drive. Note that VSL is designed to slow down drivers' speeds prior to their approaching of the congestion area (i.e. merging/diverging area). The VSL signs during the experimental period were located 800 feet upstream of two detected congestion bottlenecks, as shown in Figure 6(B).

The evaluation period was from 6:00–8:00 AM, which corresponds to the morning peak period. As shown in Figure 6(A), the high-speed traffic, when encountering the downstream congestion, drops its speed rapidly, causing a significant shockwave impact.

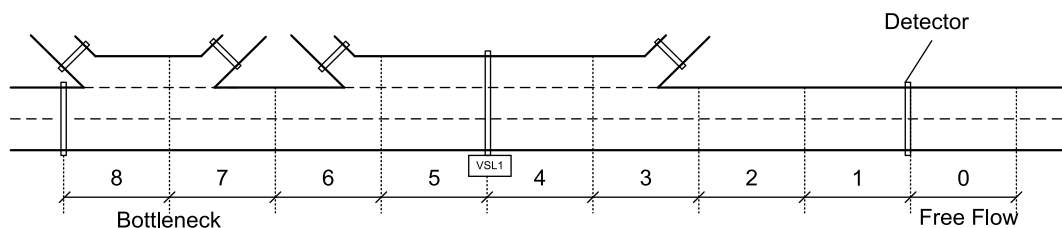
As shown in Figures 7(A)–(D), around 55% of traffic flows came from the upstream segment and the rest were from the MD 713 and 295 N on-ramp. Also, about 15% of the approaching flows took the route via bottleneck segment to the 295 S off-ramp, and the remaining 85% flows entered the downstream freeway.

5.2. Model calibration

The macroscopic model presented in Section 3 includes several parameters, which may be location-dependent. To ensure the key prediction accuracy, this study has calibrated these parameters for the target freeway segment. The parameters need to be calibrated includes the following: jam traffic



(A). Spatial evolution of traffic flow speeds on the target MD-100 segment



(B). Illustration of freeway segmentation and VSL location

Figure 6. (A) Spatial evolution of traffic flow speeds on the target MD-100 segment. (B) Illustration of freeway segmentation and variable speed limit location.

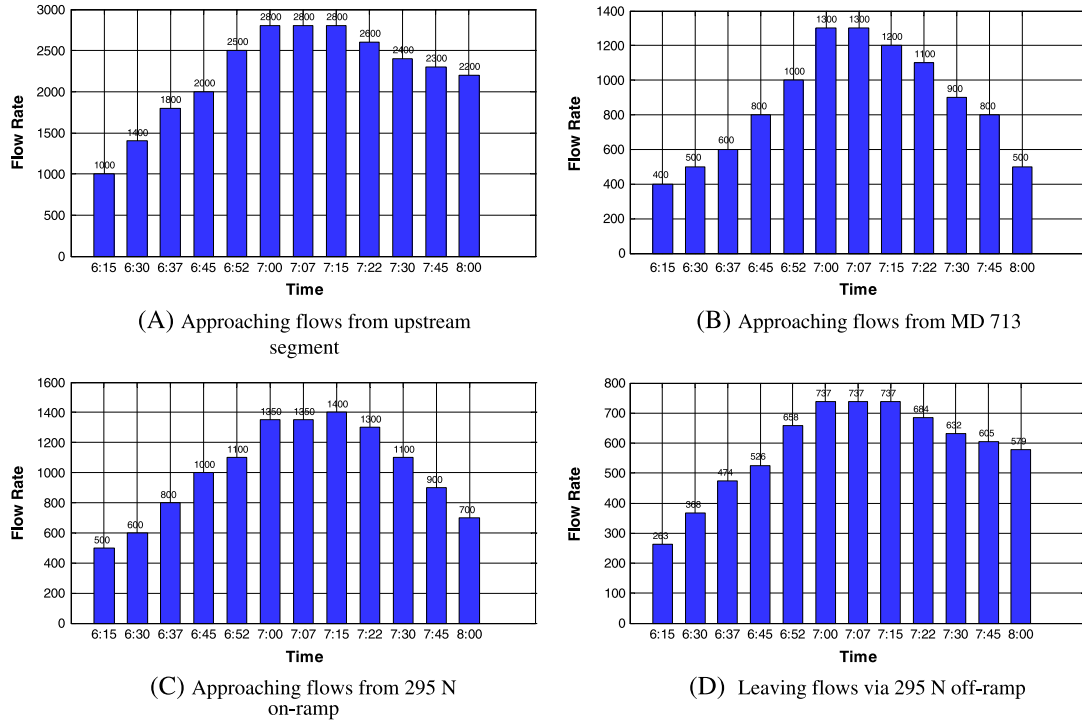


Figure 7. (A) Approaching flows from upstream segment. (B) Approaching flows from MD 713. (C) Approaching flows from 295 N on-ramp. (D) Leaving flows via 295 N off-ramp.

density d_j , critical traffic density d_C , free-flow speed u_f , and traffic model parameters v, τ, κ, a . To minimize the difference between detector measurement and model prediction results, the calibration objective is set to minimize the performance index defined in the succeeding text:

$$Min PI = \sum_i \sum_k \left[\left| \frac{q_i^{measured}(k) - q_i^{predicted}(k)}{q_i^{measured}(k) + q_i^{predicted}(k)} \right| + \left| \frac{u_i^{measured}(k) - u_i^{predicted}(k)}{u_i^{measured}(k) + u_i^{predicted}(k)} \right| \right] \quad (21)$$

One can then apply genetic algorithm to search the optimal values of those parameters. The calibration results are listed as follows:(Table I)

For performance evaluation, the micro-simulation software VISSIM, is used as an unbiased platform to test the proposed models. Similarly, the key parameters in VISSIM are calibrated with the field data. For the car-following parameters, the maximum look ahead distance was calibrated to be 1000 feet, and the CC1 (headway time) was set as 0.80 second. Lane-changing parameters were also calibrated, where the maximum deceleration is -20.11 ft/s^2 for own and -19.85 ft/s^2 for trailing vehicle; the accepted deceleration is -8.27 ft/s^2 and -6.63 ft/s^2 for own and trailing vehicle, respectively; the waiting

Table I. The calibration results of parameters.

Parameters	Calibrated values
d_j (veh/lane/km)	120
d_C (veh/lane/km)	30
u_f (km/hour)	100
v (km^2/hour)	55
τ (seconds)	36
κ (veh/km)	40
a	2.0

time before diffusion is 90 seconds. To simulate the on-line VSL control with the proposed proactive algorithms, this study has developed a VB.NET program to capture the online interaction between execution of the control algorithm and the time-varying traffic conditions. This mechanism has been programmed to enable our developed optimal VSL module to communicate with VISSIM during every simulation interval. Also note that the compliance rate of VSL is assumed to be 100% in this study.

To compare the proposed VSL models with No-control scenario, this study has designed the following four scenarios:

- BASIC-TTT: the basic proactive model with the objective of total travel time minimization;
- KF-TTT: the enhanced proactive model with the objective of total travel time minimization;
- BASIC-SV: the basic proactive model with the objective of speed variance minimization; and
- KF-SV: the enhanced proactive model with the objective of speed variance minimization.

In the models enhanced with the Kalman Filter, the deviation of measurement errors for the flow rate and speed are selected as follows:

$$\begin{aligned} D(\varepsilon_i^q(k)) &= 50 \text{ veh/h}, & D(r_i^q(k)) &= 50 \text{ veh/h}; \infty \\ D(s_i^q(k)) &= 50 \text{ veh/h}, & D(\varepsilon_i^u(k)) &= 5 \text{ km/h}; \end{aligned}$$

The deviation of prediction errors for the flow rate and speed are assumed to be

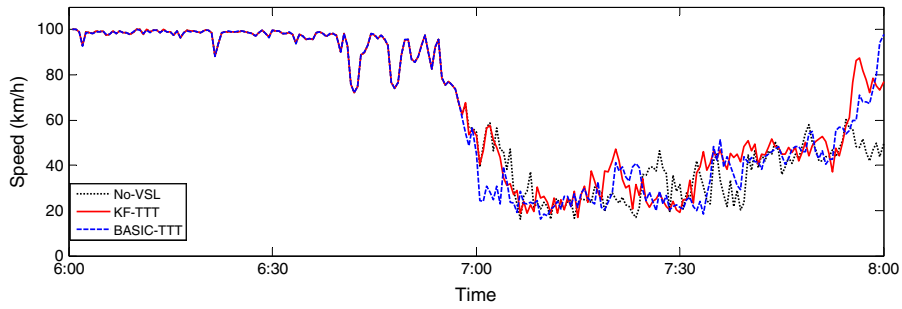
$$D(\zeta_i^q(k)) = 250 \text{ veh/h}, \quad D(\zeta_i^u(k)) = 10 \text{ km/h}.$$

5.3. Analysis of experimental results

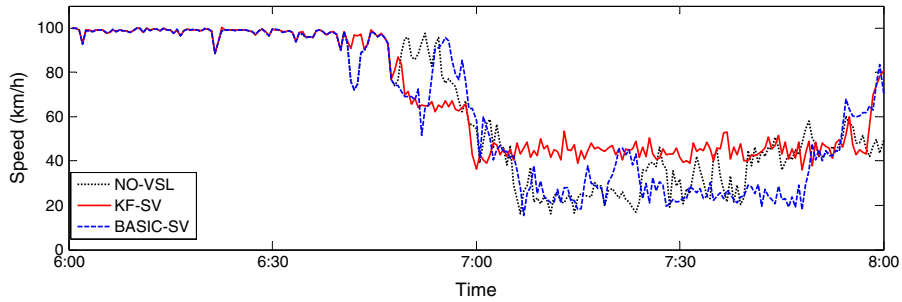
Based on the objective of minimizing the total travel time, Figure 8(A) shows the distribution of mean speeds at the bottleneck under BASIC-TTT, KF-TTT, and No-control scenario, revealing that the speeds under different scenarios are identical during the first hour (6:00–7:00 AM) due to the light traffic condition. However, during the peak hour (7:00–8:00 AM), the traffic demands increase significantly and result in the downstream congestion. Comparing these three scenarios, one can observe that both BASIC-TTT and KF-TTT can slightly offer a higher speed during the congestion period (7:15–7:45 AM), and recover the dropped speed more quickly at the rest period (7:45–8:00 AM) compared with the No-VSL control scenario. Also, KF-TTT can outperform BASIC-TTT (without using the Kalman Filter for update), which is due likely to its deficiency in offering an accurate traffic prediction and consequently unable to generate effective control speeds.

Figure 8(B) shows mean speed evolution with the control objective of minimizing speed variance at the bottleneck. Obviously, KF-SV is able to maintain a stable and much higher bottleneck speed, starting from beginning of the traffic congestion period (7:00–8:00 AM). Compared with the No-Control scenario, the BASIC-SV model was able to keep a higher speed at the congestion period (7:15–7:25 AM), but lost its efficiency during the remaining period. The reason, as stated previously, is that the basic model is unable to capture the rapidly changing traffic condition and to revise the speed limit in time during the on-line applications. Among all scenarios, the KF models with their proactive nature can always outperform the Basic models. Therefore, this study has further investigated the properties of these two KF models with different objective functions, and the results are shown in Figure 8 (C). The obtained values of speed limit from different scenarios over the control time period is given by Figure 9.

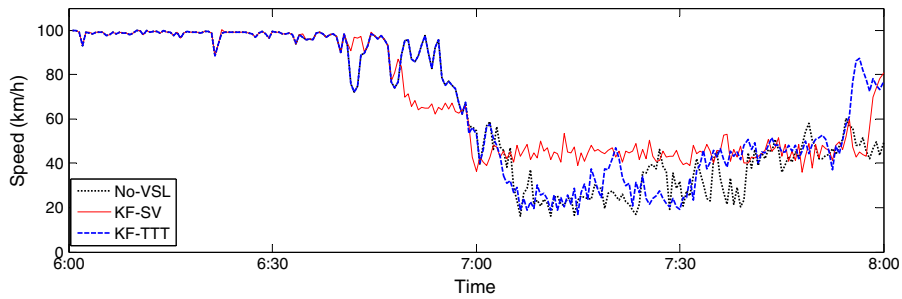
As a major measure of effectiveness (MOE) to evaluate traffic efficiency, the time-dependent travel time can clearly reflect the effectiveness of each control strategy. Figure 10(A) presents the resulting travel time from these two models with the objective of minimizing travel time and the No-VSL scenario. Notably, the travel time starts to increase when the freeway is becoming congested (after 7:00 AM). Compared with the No-control scenario, the average travel time is reduced under the KF-TTT model, demonstrating the benefits under the VSL control. However, the benefit of VSL with BASIC-TTT is not significant. The reason is that without the Kalman Filter Correction, the macroscopic traffic flow model cannot fully capture the occurrence of congestion caused by traffic weaving



(A). Bottleneck Mean speed: BASIC-TTT, KF-TTT v. s. No-VSL scenario



(B). Bottleneck Mean speed: BASIC-SV, KF-SV v. s. No-VSL scenario



(C). Bottleneck Mean speed: KF-TTT, KF-SV v. s. No-VSL scenario

Figure 8. (A) Bottleneck Mean speed: BASIC-TTT, KF-TTT versus No-VSL scenario. (B) Bottleneck Mean speed: BASIC-SV, KF-SV versus No-VSL scenario. (C) Bottleneck Mean speed: KF-TTT, KF-SV versus No-VSL scenario.

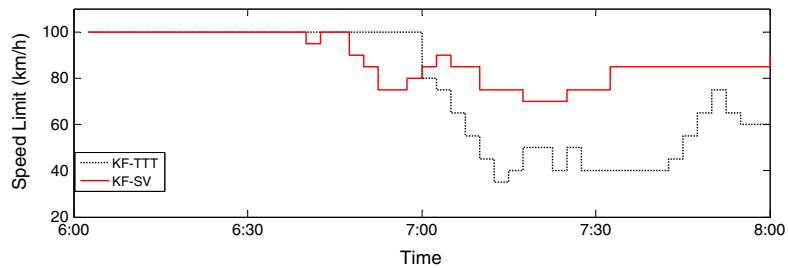
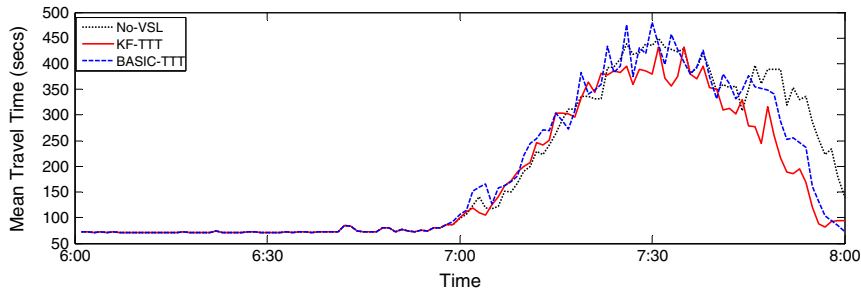


Figure 9. The values of speed limit by different variable speed limit control models.

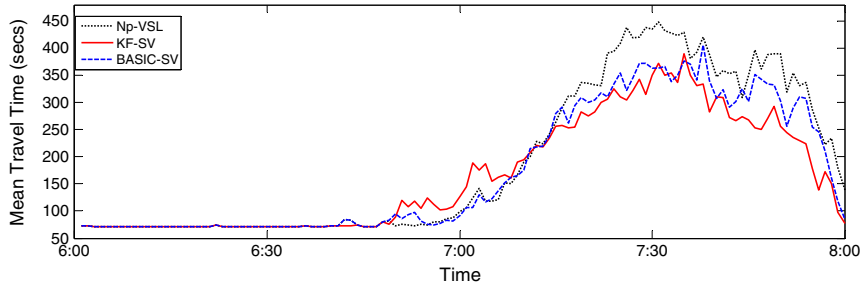
effect at the downstream bottleneck. From Figure 10(B), it is clear that both speed variance minimization models can reduce the travel time during the congested period (7:00–8:00 AM). Also, the KF-SV model clearly outperforms the BASIC-SV model.

A further comparison between two KF models is shown in Figure 10(C). Note that during the period 6:45–7:15 AM, the KF-TTT model produces a lower travel time than the KF-SV model. However, as

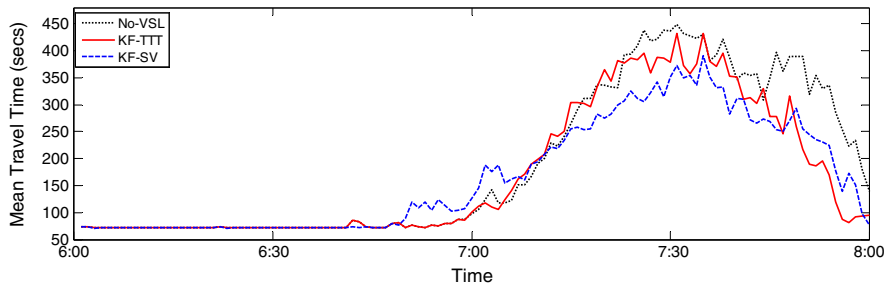
OPTIMAL VARIABLE SPEED CONTROL SYSTEM



(A). Time-dependent travel time: BASIC-TTT, KF-TTT v. s. No-VSL scenario



(B). Time-dependent travel time: BASIC-SV, KF-SV v. s. No-VSL scenario



(C). Time-dependent travel time: KF-TTT, KF-SV v. s. No-VSL scenario

Figure 10. (A) Time-dependent travel time: BASIC-TTT, KF-TTT versus No variable speed limit (VSL) scenario. (B) Time-dependent travel time: BASIC-SV, KF-SV versus No-VSL scenario. (C) Time-dependent travel time: KF-TTT, KF-SV versus No-VSL scenario.

the congestion increases from 7:15 AM, the KF-SV model begins to show better performance. To understand this interesting finding, we further analyzed the simulation process and found out that the KF-SV model is more sensitive to the change in traffic conditions, and it can immediately adjust the speed limit in advance even during the moderate congested period. The capability to adjust speed in time can reduce the flow rate to the downstream segments and consequently mitigate the potential shockwave impact.

Table II summarizes the MOEs for all scenarios. To prevent the randomness of results, the data have been averaged over five simulation replications. Moreover, to distinguish the performance between the

Table II. Performance comparison between different scenarios.

Scenario	6:00–8:00		7:00–8:00		6:00–8:00		7:00–8:00		Speed SD (km/hr)	
	Ave. # of stops		Ave. # of stops		Ave. travel time (s)		Ave. travel time (s)			
No-VSL	6.3	/	10.5	/	214.6	/	306.5	/	19.3	/
BASIC-TTT	5.6	–11.1%	9.2	–12.4%	208.7	–2.7%	294.9	–3.8%	18.4	–4.7%
KF-TTT	4.7	–25.4%	7.8	–25.7%	191.4	–10.8%	267.7	–12.7%	17.1	–11.4%
BASIC-SV	4.8	–23.8%	7.9	–24.8%	193.2	–10.0%	270.0	–11.9%	17.5	–9.3%
KF-SV	4.1	–34.9%	6.5	–38.1%	185.0	–13.8%	250.1	–18.4%	16.4	–15.0%

Ave., average; VSL, variable speed limit; TTT, total travel time minimization; SV, speed variance.

congested (7:00–8:00 AM) and uncongested periods (6:00–7:00 AM), Table II shows the overall results over the entire period and over the congested period. Notably, all proposed models can yield significant reduction in total travel time, vehicle stops and standard deviation of speed. Among those four, KF-SV model is the best one, which yields a reduction of 36.6% on the vehicle stops, 14.7% on the average travel time and 4.7% on speed difference during the 2-hour period. KF-TTT model with its dynamic update function outperforms BASIC-SV, and achieves a reduction in vehicle stops, travel time, and speed variance, respectively, by 25.4%, 10.8%, and 11.4%.

In brief, one can tentatively reach the following preliminary conclusions from the aforementioned extensive experimental analysis:

- A proper VSL system can effectively reduce the number of stops and travel time over a recurrently congested freeway segment.
- The macroscopic traffic flow model cannot fully capture the occurrence of congestion caused by traffic weavings, as reflected by the travel time and number of stops produced by the models without KF.
- The accuracy of the predicted traffic congestion can significantly affect the effectiveness of a VSL control system, as evidenced by the superior performance of those two models with an embedded KF functions.
- Also, speed variance minimization seems to be a better control objective, as the speed data is directly measurable from detectors and is the most sensitive variable to the VSL control. And the speed variance minimization model is less sensitive to the prediction accuracy, as reflected in the performance evaluation results.

Note that drivers' compliance rate is assumed as 100% in this case study, which is often not true in practice. According to the field observations from literature, the studies have investigated a wide range of drivers' compliance rate from 20% to 80% at different sites. Hence, to ensure the operational effectiveness of a VSL control system, one shall account for the impact caused by the compliance rate in practice. One possible way is to incorporate a real-time feedback control function to dynamically adjust the obtained optimal speed limit based on the detected compliance rate. However, how to model such impacts in the optimization model is still a challenge issue, which might be one of our primary future tasks.

6. CONCLUSIONS AND FUTURE RESEARCH

In summary, this study has proposed two proactive VSL control models for use on recurrently congested freeway segments. The basic proactive model used the embedded traffic flow relations to predict the evolution of congestion pattern and compute the optimal speed limit. To contend with the difficulty in capturing driver responses to VSL control, this study has also proposed an advanced model with an embedded Kalman Filter function. Both models have been investigated with different traffic conditions and control objectives. The results of extensive VISSIM simulation have revealed that both proactive VSL control models can significantly reduce the travel time and the number of vehicle stops over recurrent bottleneck locations at MD 100, and the one using minimizing speed variance as its control objective clearly outperforms other models, as reflected in the performance evaluation results.

Despite the promising performance of our proposed models at this exploratory stage, the authors fully recognize that much remains to be carried out on this subject. One of our on-going tasks is to calibrate drivers response parameters based on more field data. Also, the sensitivity of model performance to the traffic measurement errors is not answered yet in this study. Other on-going research tasks associated with VSL implementation include: exploring the potential of using control objectives to provide trade-off between operation and safety performance, identification of optimal detector locations for updating traffic conditions, and assessment of the road emissions produced by different VSL control systems.

7. LIST OF ABBREVIATIONS

VSL	variable speed limit
ITS	intelligent transportation system
MPC	model predictive control
CTM	cell transmission model

REFERENCES

1. Papageorgiou M, Hadj-Salem H, Blosseville JM. ALINEA: A local feedback control law for on-ramp metering. *Transportation Research Record* 1991; **1320**:58–64.
2. Papageorgiou M, Hadj-Salem H, Middelham F. ALINEA local ramp metering: summary of field results. *Transportation Research Record* 1997; **1603**:90–98.
3. Cambridge Systematics. Twin cities ramp meter evaluation: final report. Minnesota Department of Transportation, 2001.
4. Paesani G, Kerr J, Perovich P, Khosravi E. System wide adaptive ramp metering in southern California. *Proceedings of the ITS America 7th Annual Meeting*, 1997.
5. Steel P, McGregor RV, Guebert AA, McGuire TM. Application of variable speed limits along the Trans Canada Highway in Banff National Park. *Proceedings of the Annual Conference of the Transportation Association of Canada*, 2005.
6. Ulfarsson GF, Shankar VN, Vu P. The effect of variable message and speed limit signs on mean speeds and speed deviations. *International Journal of Vehicle Information and Communication Systems* 2005; **1**:69–87.
7. Anund A, Ahlström C, Almqvist S, Yahya MR. Evaluation of local ITS solutions in urban areas. *VTI Report*, 2009.
8. Lyles R, Taylor WC, Grossklaus J. Field test of variable speed limits in work zones (in Michigan). Michigan Department of Transportation, 2003.
9. Lin PW, Kang KP, Chang GL. Exploring the effectiveness of variable speed limit controls on highway work-zone operations. *Journal of Intelligent Transportation System* 2004; **8**(3):155–168.
10. Kang KP, Chang GL, Zou N. Optimal dynamic speed-limit control for highway work zone operations. *Transportation Research Record* 1877; **2004**:77–84.
11. Kang KP. Development of optimal control strategies for freeway work zone operations. Ph. D. dissertation, Department of Civil & Environmental Engineering, University of Maryland, 2006.
12. Kwon E, Brannan D, Shouman K, Isackson C, Arseneau B. Development and field evaluation of variable advisory speed limit system for work zones. *Transportation Research Record* 2015; **2007**:12–18.
13. Fudala NJ, Fontaine MD. Interaction between system design and operations of variable speed limit systems in work zones. *Transportation Research Record* 2010; **2169**:1–10.
14. Abdel-Aty M, Dilmore J, Hsia L. Applying variable speed limits and the potential for crash migration. *Transportation Research Record* 1953; **2006**:21–30.
15. Abdel-Aty M, Cunningham RJ, Gayah VV, Hsia L. Dynamic variable speed limit strategies for real-time crash risk reduction on freeways. *Transportation Research Record* 2008; **2078**:108–116.
16. Hegyi A. Model predictive control for integrating traffic control measures. Ph. D. dissertation, Netherlands TRAIL Research School, 2004.
17. Hegyi A, De Schutter B, Hellendoorn J. Optimal coordination of variable speed limits to suppress shock waves. *IEEE Transactions on Intelligent Transportation Systems* 2006; **6**:102–112.
18. Papageorgiou M, Kosmatopoulos E, Papamichail I. Effects of variable speed limits on motorway traffic flow. *Transportation Research Record* 2008; **2047**:37–48.
19. Carlson RC, Papamichail I, Papageorgiou M, Messmer A. Optimal motorway traffic flow control involving variable speed limits and ramp metering. *Transportation Science* 2010; **44**:238–253.
20. Carlson RC, Papamichail I, Papageorgiou M. Local feedback-based mainstream traffic flow control on motorways using variable speed limits. *IEEE Transactions on Intelligent Transportation Systems* 2011; **12**:1261–1276.
21. Hadiuzzaman M, Qiu TZ. Cell transmission model-based variable speed limit control for freeways. *Proceedings of Transportation Research Board 91st Annual Meeting*, 2012.
22. Talebpour A, Mahmassani HS, Hamdar SH. Speed harmonization: effectiveness evaluation under congested conditions. *Proceedings of Transportation Research Board 92nd Annual Meeting*, 2013.
23. Smulders S. Control of freeway traffic flow by variable speed signs. *Transportation Research Part B* 1990; **24**:111–132.
24. Hegyi A, Hoogendoorn SP. Dynamic speed limit control to resolve shock waves on freeways – Field test results of the SPECIALIST algorithm. *Proceedings of the 13th IEEE Conference on Intelligent Transportation Systems*, 2010.
25. Weikl S, Bogenberger K, Bertini RL. Traffic management effects of variable speed limit system on a German Autobahn empirical assessment before and after system implementation.
26. Chang GL, Park SY, Paracha J. Intelligent transportation system field demonstration: integration of variable speed limit control and travel time estimation for a recurrently congested highway. *Transportation Research Record* 2011; **2243**:55–66.
27. Messner A, Papageorgiou M. METANET: A macroscopic simulation program for motorway networks. *Traffic Engineering & Control* 1990; **31**(8–9):466–470.
28. Wang Y, Papageorgiou M. Real-time freeway traffic state estimation based on extended Kalman filter: a general approach. *Transportation Research Part B* 2005; **39**:141–167.